



Design exploration of hypersonic vehicle airframe and air-breathing engine using deep-learning flowfield prediction

Chihiro Fujio¹, Hideyuki Taguchi²

Abstract

Hypersonic airbreathing vehicle is a promising candidate for high-speed point-to-point transportation and first stage of space transportation system. The airbreathing engine is often mounted to utilize the compression through the vehicle body. However, the design of airbreathing engine and vehicle airframe are often conducted in a separated manner. This may limit the performance of scramjet engine and vary the vehicle longitudinal stability. The present study aims to develop the methodology for simultaneous design of vehicle airframe and scramjet engine. Deep-learning perdiction is employed to accurately evaluate scramjet flowfields and local surface inclination method is for vehicle airframe. The developed approach has been employed for multi-objective design optimization of hypersonic airbreathing vehicles, demonstrating the co-design of scramjet engine and vehicle airframe.

Keywords: airbreathing hypersonic vehicle, scramjet, deep learning

1. Introduction

Hypersonic vehicles with air-breathing engines are a promising candidate for high-speed point-to-point transportation as well as space transportation. Various hypersonic airplanes have been proposed and investigated until today, including HYTEX, which is equipped with pre-cooled turbojet engines, proposed by JAXA [1, 2], and VISR, which uses scramjet engines, proposed by an Australian company Hypersonix [3]. Designing such hypersonic air-breathing vehicles requires appropriate integration of a vehicle airframe with air-breathing engines to simultaneously satisfy the requirement for flight stability and efficient thrust generation. While it have not been a significant problem in case with the design of conventional airplanes, this problem is caused by the requirement from high-speed airbreathing engines to effectively utilize the body surface to compress the incoming airflow.

However, the current design process of hypersonic air-breathing vehicles is usually divided into airframe design and engine design because the simultaneous design of vehicle airframe and engine is complicated due to a large number of design parameters, consideration of engine operation with complicated aero-thermodynamics, and necessity of evaluations at various flight conditions, attitudes, and engine operations. The process limits the performance of hypersonic vehicles and may incur the risk of design modifications, repeatedly. Several preseding studies have taken the influence of engine operation on vehicle stability into account. Bowcutt have reported a multidisciplinary optimization study of airbreathing hypersonic vehicle [4]. In this study, pitching moment caused by scramjet has been considered to evaluate the longitudinal stability of the vehicle, but the scramjet flowpath has been fixed. Riggins and Bowcutt have also been developed analytical approach to design hypersonic vehicle considering the mission of the vhielce. However, it is difficult to accurately evaluate scramjet performance [5]. Dalle *et al.* reported similar methodology yet the approach allows to calculate combustion efficiency based on a fuel-air mixing model [6].

Although research effort has been paied to improve the design approach of hypersonic airbreathing vehicle, it is yet to be a problem that the accurate evaluation of engine performance and its influence on vehicle characteristics. The present study, thus, report a new approach to simultaneously evaluate vehicle

¹Japan Aerospace Exploration Agency, fujio.chihiro@jaxa.jp

² Japan Aerospace Exploration Agency, taguchi.hideyuki@jaxa.jp

and engine flowfields by employing a deep-learning technique. Surface pressure ans shears stress profiles are predicted using deep-learning flowfield prediction for two-dimensional hydrogen-fueled scramjet with enabling accurate prediction over various geometries and operating condition (angle of attack and injection pressure). A multi-objective design optimization of airbreathing hypersonic vehicles has been conducted by combining the deep-learning model for engine and local surface inclination method for vehicle aerodynamics.

2. Methodology

2.1. Integrated evalutaion of airframe and airbreathing engine

2.1.1. Overview

The present study develops an approach for evaluating airframe aerodynamic characteristics and engine performance simultaneously combining a low-fidelity approach for vehicle aerodynamics and a deep-learning approach for engine operations. This approach allows to evaluate vehicle aerodynamic characteristics considering influences of engine operation within a few seconds. Overview of the evaluation approach is schematized in Fig. 1, including 4 parts, (1) modeling, (2) surface mesh generation, (3) evaluation of pressure coefficients on vehicle surface, and (4) evaluation of pressure coefficients on scramjet engine surface. Aerodynamic coefficients are then calculated based on the surface pressure coefficients. This framework mainly relies on a local surface inclination (LSI) method framework UNLSI, which has been developed at the University of Tokyo [7], and the capability of evaluating pressure coefficients under engine operation is added by employing deep-learning flowfield prediction techniques.

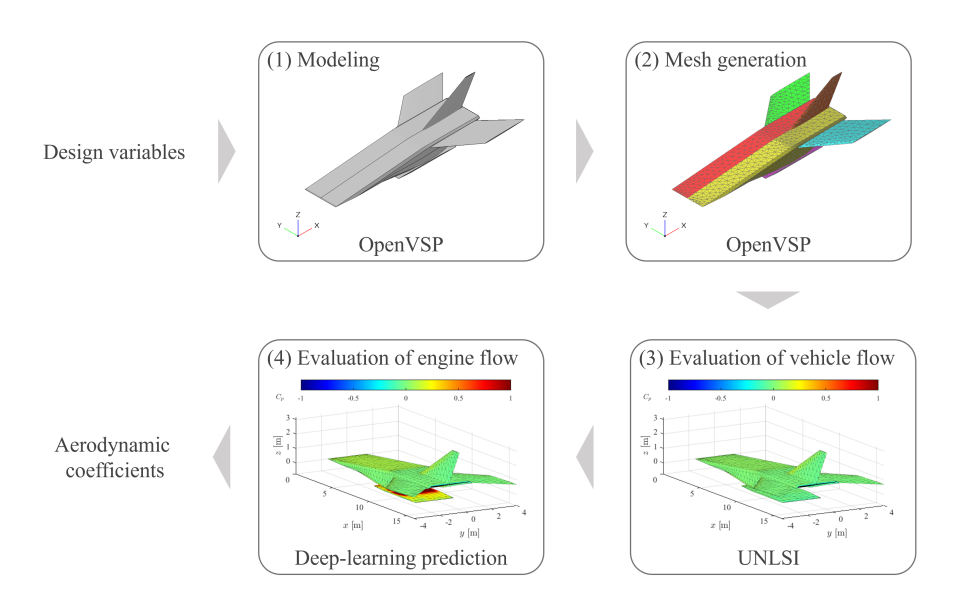


Fig 1. Overview of approach for Integrated evaluation of vehicle aerodynamics and engine propulsion

The 3D modeling and surface mesh generation has been conducted using an open source parametric geometry and analysis tool OpenVSP [8]. This allows to generate vehicle airframe shape in a parametric manner based on script files. Surface mesh is generated using OpenVSP and then is used for both LSI analysis and deep-learning flow prediction. LSI analysis is performed for whole of the airframe but the pressure coefficients of the fuselage and engine is replaced by those evaluated by using deep-learning flowfield prediction.

2.1.2. Evaluation of vehicle aerodynamics

Local surface inclination method has been employed to evaluate vehicle aerodynamic characteristics without considering the effect of engine operation on vehicle aerodynamics. The calculation of pressure coefficient is conducted by using Tangent-Cone method for compression waves and Prandtl-Meyer

method for expansion waves.

Angles between flow and vehicle surface is culculated as below:

$$\delta = \arccos\left(\frac{\mathbf{n} \cdot \mathbf{V_{inf}}}{\mathbf{V_{inf}}}\right) \tag{1}$$

where $\bf n$ is a vector nomal to surface and $\bf V_{inf}$ is a mainstreem velocity vector. In case with $\delta \geq 0$, Tangent-Cone method is employed to estimate pressure coefficients usign following equations:

$$M_a = 1.090909 M_{inf} + \exp\left(-1.090909 M_{inf} \sin \delta\right) \tag{2}$$

$$C_{p} = \frac{2\sin^{2}\delta}{1 - \frac{1}{4}\left(M_{a}^{2} + 5\right)/\left(6M_{a}^{2}\right)} \tag{3}$$

In case with $\delta < 0$, Prandtl-Meyer method is employed and expansion waves are calculated as follows:

$$\nu\left(M\right) = \sqrt{\frac{\gamma+1}{\gamma-1}}\arctan\left(\sqrt{\frac{\gamma-1}{\gamma+1}\left(M^2-1\right)}\right) - \arctan\left(\sqrt{(M^2-1)}\right) \tag{4}$$

$$\nu\left(M_{inf}\right) = \nu\left(M_{l}\right) - \delta \tag{5}$$

where M_l is a local Mach number for each panel. Pressure coefficients are calculated using following equations with an assumption of adiabatic process:

$$\frac{T_l}{T_{inf}} = \frac{2 + (\gamma + 1) M_{inf}^2}{2 + (\gamma + 1) M_l^2}$$
 (6)

$$\frac{p_l}{p_{inf}} = \frac{T_l}{T_{inf}}^{\frac{\gamma}{\gamma - 1}} \tag{7}$$

$$C_p = \frac{2\left(\frac{p_l}{p_{inf}} - 1\right)}{\gamma M_{inf}} \tag{8}$$

2.1.3. Evaluation of engine flowfield

Fast and accurate evaluation of engine flowfields has been conducted by employing deep-learning flowfield prediction. The present study employes a multi-layer perceptron (MLP)-based flowfield prediction appraoch proposed by Fujio and Ogawa [9]. While the original model employs to predict whole of the flowfields, this study employ to only predict wall pressure coefficients and skin friction coefficients. Figure ?? schematizes the model configuration. The MLP model consists of an input layer which passes input data, hidden (fully-connected) layers which plays a main role of data fitting, and an output layer which outputs prediction results from MLP. In the present study, 8 variables are feed as input data including 4 design variables, 2 control variables, and coordinate on fuselage surface, and 3 variables, static pressure and wall shear stress τ_x and τ_y are provided by the MLP model. In the present study, the number of hidden layers is set to be 5 and the size of each hidden layer to be 1024, and Relu function is used for the activation function, based on the preceding studies [10, 11]. The training of the model is conducted by using a gradient-based optimization method Adam (adaptive momentum estimation) with their default values of hyperparameters [12]. Mean square error is selected as the loss function with Dropout to mitigate the risk of overfitting and increase the prediction accuracy. Dropout rate is set to be 5% in the present study. 1000 CFD results, which are obtained via Latin Hypercube sampling, are prepared for training the MLP model and 100 CFD results for validating the model prediction accuracy. CFD solved RANS equations with SST $k-\omega$ turbulence model [13]. Supersonic combustion of hydrogen is calculated using a reduced reaction mechanism proposed by Boivin et al. [14]. The model configuration and setups for model training are summarized in Table 1.

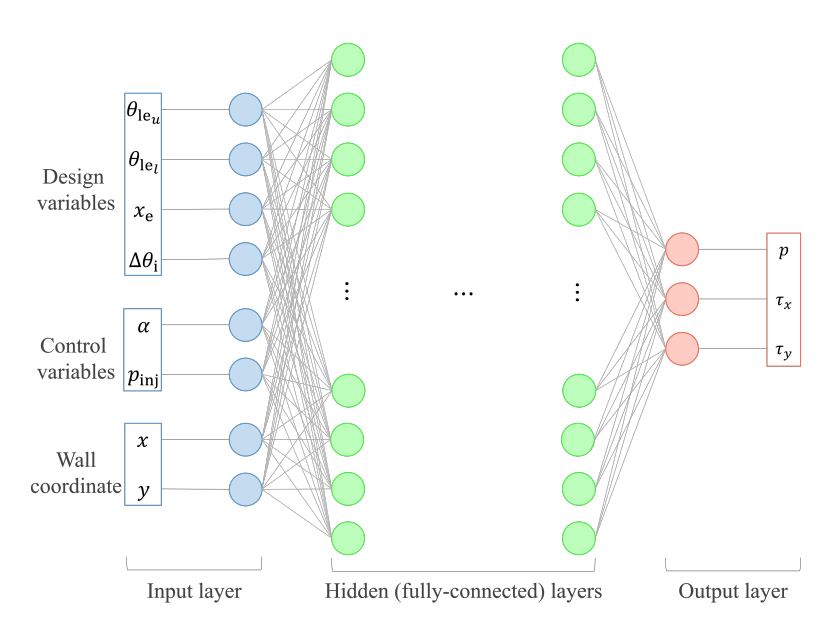


Fig 2. Schematic of present flowfield prediction model

Table 1. Model configuration and setups

Number of layers	5
Number of units	1024
Dropout rate	5%
Activation function	Relu
Optimizer	Adam [12]
Max epoch	1000
Learning rate	10^{-5}

2.2. Configuration

The present study considers a wedge-shaped waverider with a scramjet engine which is mounted on the vehicle bottom. The vehicle consists of wedge-shaped fuselage, a main wing with dehedral and sweepback angle, and a vertical tail. Parameterization of the vehicle geometry is summarized in Fig. 3. The planform is determined by root chord of main wing C_r , sweepback angle Λ , main wing span b_w , taper ratio λ , and fuselage span b_b . The variables of cross section includes vehicle upper-wall leading-edge angle $\theta_{le,u}$, lower-wall leading-edge angle $\theta_{le,l}$, engine location x_e , and increment of intake ramp angle $\Delta\theta_i$. In the present study, main wing dehidral Γ has also been considered. The shape of the vertical tail is fixed in the present study because it does not largely influence longitudinal stability.

The flight condition is set to be Mach 5 at the dynamic pressure of 50 kPa as a basic scramjet flight condition. The other parameters are summarized in Table. 2.

Table 2. Mean absolute errors of wall-profile prediction

Mach number	Dynamic pressure	Altitude	Static pressure	Static temperature
5	50 kPa	24.3 km	2857.1 Pa	220.8 K

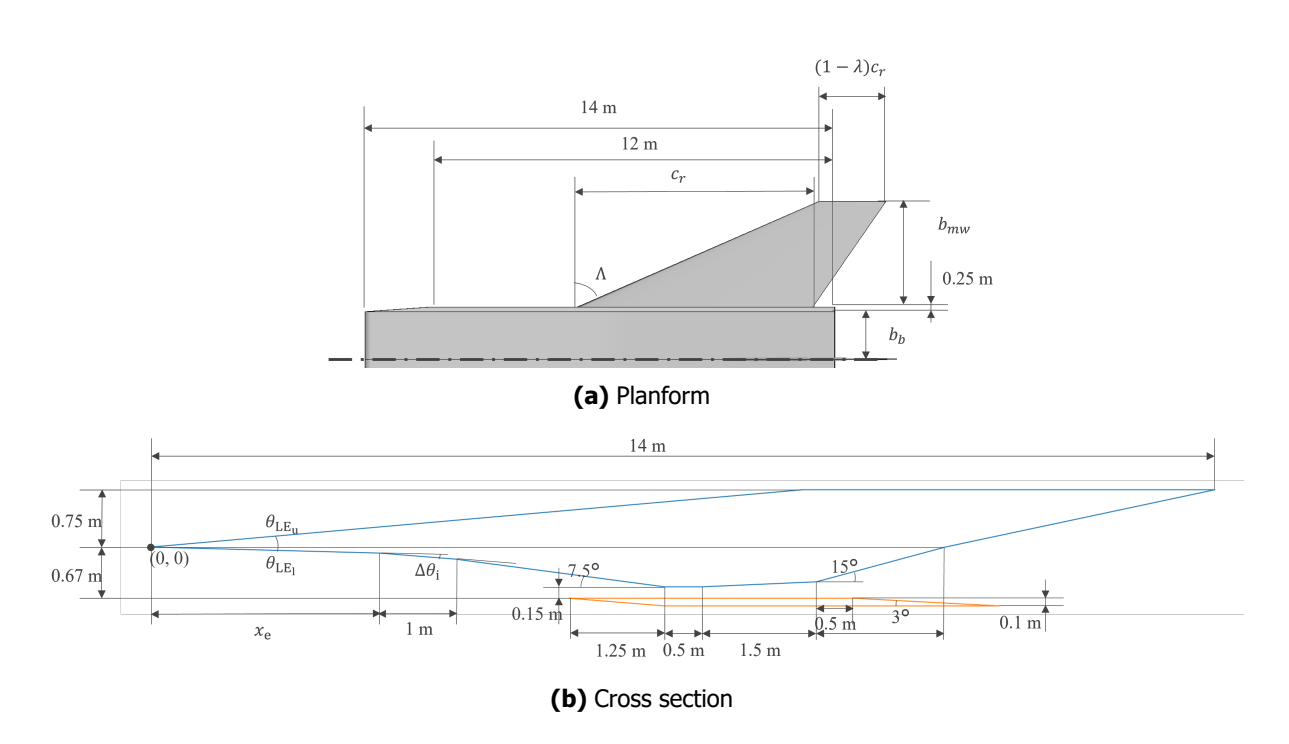


Fig 3. Parameterization of wedge-shaped waverider

2.3. Optimization

2.3.1. Optimization problem

Multi-objective optimization is conducted to simultaneously optimize both airframe and scramjet engine of a hypersonic cruise vehicle. The present study considers lift coefficient and fuel mass flow rate at the cruise (trim flight) condition as the objective functions. Lift coefficient is employed to maximize the cruise payload mass and fuel mass flow rate is minimized to increase cruise range for a given amount of fuel. Constraint functions are determined to ensure stable cruise flight. Longitudinal static stability against angle of attack is taken into account around the trim condition. The solutions that do not have trim angle of attack and injection pressure have also been considered as infeasible solutions. The optimization problem is summarized below:

 $\begin{array}{ll} \textit{Minimize:} & -C_L \\ & \dot{m}_f \\ \textit{Subject to:} & \max\left(\frac{\partial C_M}{\partial \alpha}\right) < 0 \text{ at cruise injection pressure} \\ & \min\left(|C_D|\right) < 10^{-4} \text{ at trim conditions} \\ & \min\left(|C_M|\right) < 10^{-4} \end{array}$

 $C_L > 0$ at cruise condition

In the present study, 10 geometric parameters shown in Fig. 3 have been considered as the decision variables. The ranges of decision variables are summarize in Table 3.

2.3.2. Optimization method

The present study employs a genetic algorithm, NSGA-II proposed by Deb *et al.* [15] to deal with multi-objective optimization problem and explore a wide variety of Pareto optimal solutions. NSGA-II determines the decision variables based on the values of objective functions and the control variables (angle of attack and fuel injection pressure) for each individual are determined through a gradient-based optimization. The optimization loop is schematized in Fig. 4. The inner optimization is conducted

Name	Variable	Unit	Lower bound	Upper bound
Upper-wall leading-edge angle	$\theta_{le,u}$	deg	5	10
Lower-wall leading-edge angle	$ heta_{le,l}$	deg	0	3
Engine location	x_e	m	2	4
Intake ramp angle increment	$\Delta \theta_i$	deg	2.5	5
Body span	b_b	m	1	2.5
Dehidral	Γ	deg	-5	5
Root chord	C_r	m	3	5.5
Wing span	b_w	m	0.5	3.5
Sweepback angle	Λ	deg	45	60
Taper ratio	λ	-	0	0.75

Table 3. Ranges of decision variables

by using sequential quadratic programming (SQP). The ranges of control variables are summarized in Table 4

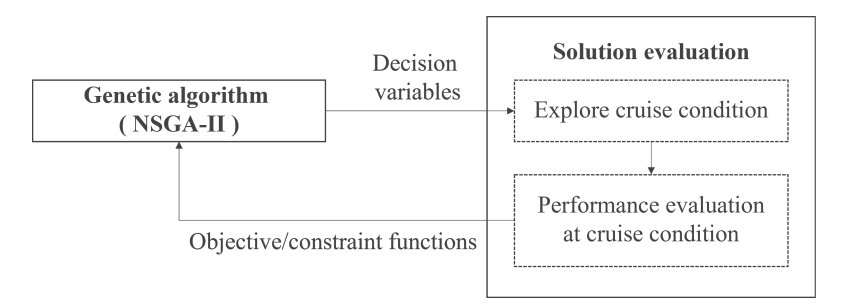


Fig 4. Schematic of optimization procedure

Table 4. Ranges of control variables

Name	Variable	Unit	Lower bound	Upper bound
Angle of attack	α	deg	0	5
Fuel injection pressure	p_{inj}	Pa	150000	450000

The evolutionary process is continued until the $50^{\rm th}$ generation with a population size of 48. Simulatd binary crossover (SBX) and polynomial mutation are employed for crossover and mutation, respectively. Both crossover index and mutation index is set to be 10 and the probility of mutation is 10% in the present study.

3. Results

3.1. Flowfield prediction

Accuracy of flowfield prediction has been assessed over 100 test data, which is not used for model training. Mean absolute errors (MAEs) of flowfield prediction has been summarized in Table 5. The predicted profiles of the case with the largest MAE of static pressure have been compared with those obtained via CFD (correct data) in Fig. 5. Even with the largest MAE, flow profiles on the vehicle surface have been accurately predicted while prediction errors have been observed around the pressure rise related to shock waves inside combustor.

Table 5. Mean absolute errors of wall-profile prediction

	p [Pa]	$ au_x$ [Pa]	$ au_y$ [Pa]
Minimum	460.0	6.59	0.737
Maximum	2513	26.80	1.443
Average	837.4	9.87	0.959

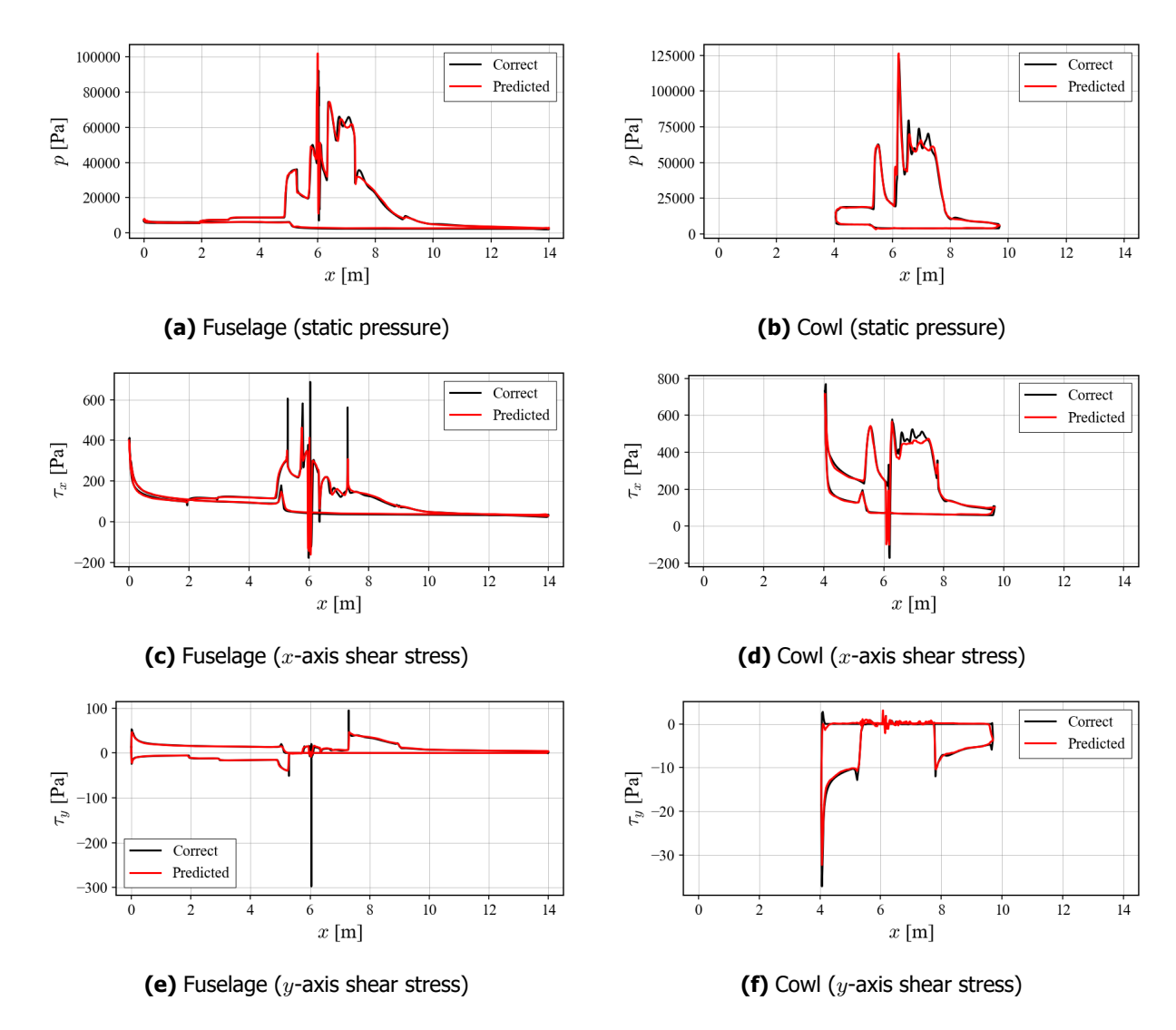


Fig 5. Comparison of pressure profiles between prediction (MLP) and correct (CFD) data

Performance parameters calculated using predicted profiles have been compared with those calculated using CFD results (correct data) in Fig. 6. All performance parameters (drag, lift, pitching moment) have been found to be estimated with a reasonable accuracy using predicted wall profiles. The coefficient of determination has also been assessed and shown in Fig. 6.

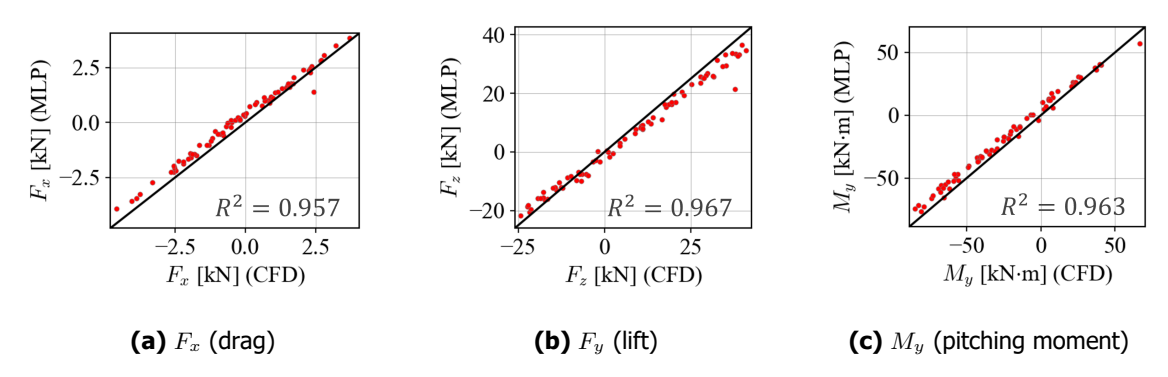


Fig 6. Comparison between predicted (MLP) and correct (CFD) performance parameters

3.2. Optimization results

3.2.1. Overview

Multi-objective design optimization has been conducted over 50 generations with a population size of 48, resulting in 33 non-dominated solutions. Figure 7 (a) displays the Pareto optimal front in the objective function, and relative values of objective functions and decision variables are shown in the form of a parallel coordinate plot in Fig. 7 (b). Additionally, fuel injection pressure and angle of attack at the cruise condition have also been shown in Fig. 7 (b). It has been observed that the non-dominated solutions have been concentrated on a part of the design space with minor variations of decision variables, as seen in Fig. 7 (b). In particular, the decision variables that determines cross-sectional shape of fuselage exists within narrow ranges for feasible and non-dominated solutions. Figure 8 shows the cross-sectional shape of fuselage for feasible and non-dominated solutions. The angle of vehicle upper surface $\theta_{le,u}$ has been settled in the vicinity of 5 deg, which is the lower bounds of the range of $\theta_{le,u}$, to be feasible solutions, because larger $\theta_{le,u}$ results in larger negative pitching moment.

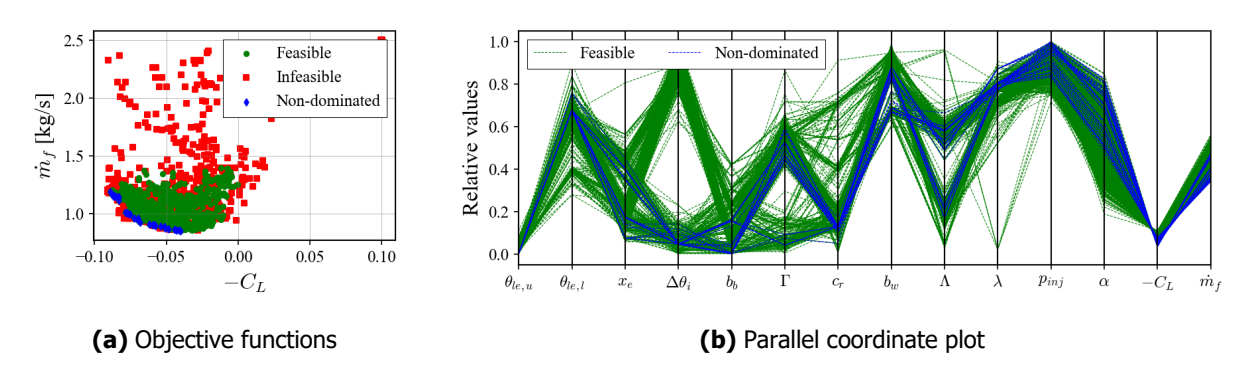


Fig 7. Overview of optimization results

Control variables (angle of attack α and injection pressure p_{inj}) at the cruise condition are displayed in Fig.9. It has been found that the variations of control variables are responsible for the variations of objective functions on the Pareto optimal front. Larger angle of attacks at trim conditions resulting in larger lift coefficients. Injection pressure directly determines the mass flow rate of fuel and is closely

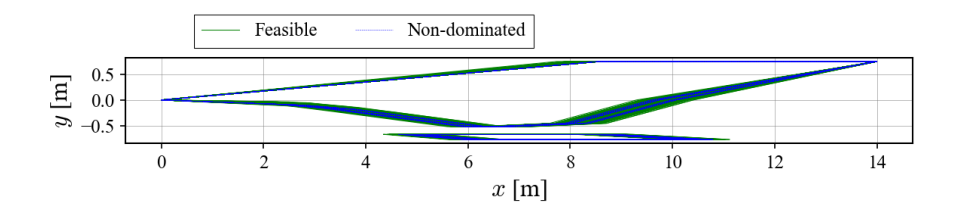


Fig 8. Cross-sectional shapes of feasible and non-dominated solutions

related to the amount of force generated via combustion. Therefore, higher injection pressure has resulted in larger fuel mass flow rate and larger lift coefficient.

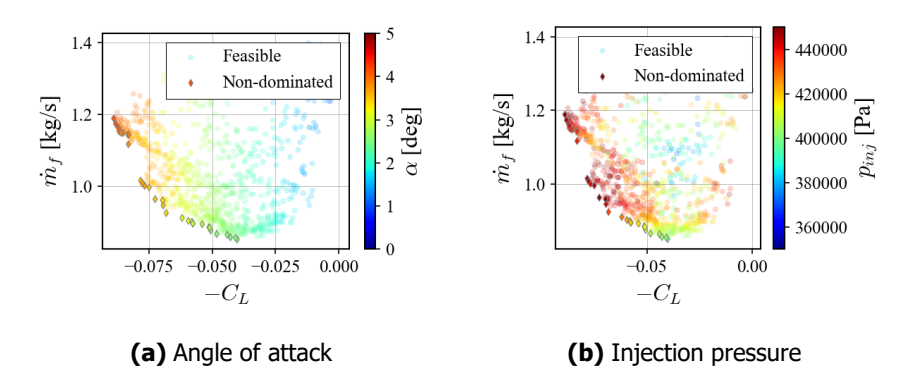


Fig 9. Control variables at trim conditions

3.2.2. Characterization of non-dominated solutions

There are two different islands of non-dominated solutions in Fig. 7 (a). Three non-dominated solutions have been selected, as seen in Fig. 10 to further investigate characteristics of non-dominated solutions. Geometries of selected solutions are displayed in Fig. 11 and the decision variables values are summarized in Table 6. Minor difference is observed for body span, wing span, sweepback angle, and dihedral. Aerodynamic coefficients over various angle of attack and injection pressure are displayed for S_1 in Fig. 12 as an example. A red dot in Fig. 12 represents the cruise condition of the vehicle. It is interesting to note that the injection angle has less influence on pitchning moment coefficients (Fig. 12 (c)), whereas drag coefficients clearly decrease as the injection pressure hence fuel mass flow rate increases (Fig. 12 (a)).

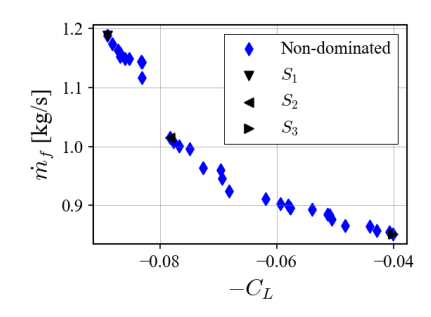


Fig 10. Clusters and selected non-dominated solutions

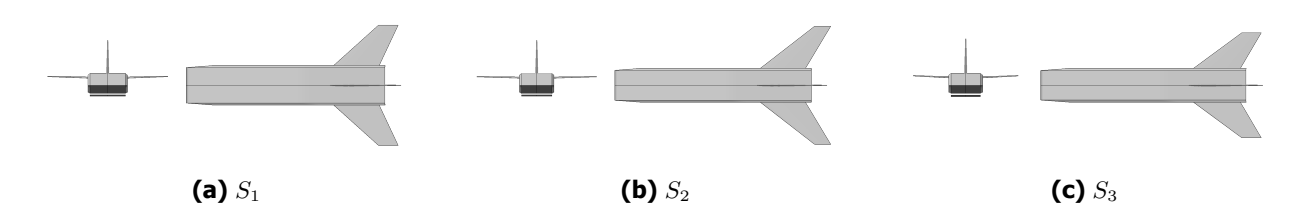


Fig 11. Objective function values of selected non-dominated solutions

 $\theta_{le,u}$ [deg] $\theta_{le,l}$ [deg] x_e [m] $\Delta\theta_i$ [deg] b_b [m] Γ [deg] C_r [m] Λ [deg] λ [-] b_w [m] 5.016 2.038 2.344 2.616 1.245 0.282 3.300 2.987 48.08 0.580 S_1 S_2 5.000 2.048 2.251 2.794 1.065 -0.3283.134 52.27 0.654 3.318 S_3 5.017 2.028 2.809 2.616 1.002 0.852 3.311 2.563 53.72 0.599

Table 6. Decision variable values of selected solutions

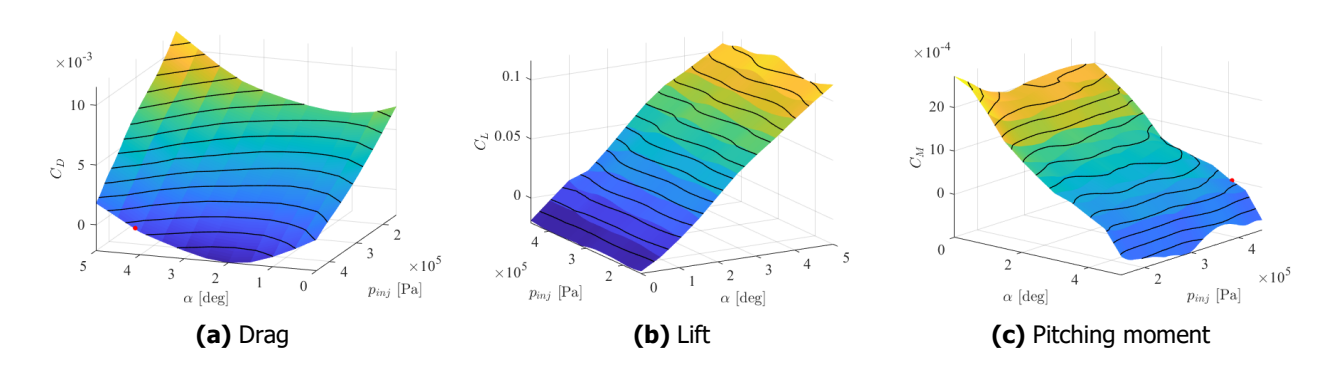


Fig 12. Aerodynamic coefficients over angle of attack and injection pressure for S_1

4. Conclusions

The present study has developed an approach to evaluate vehicle aerodynamic performance taking scramjet flowfield accurately into consideration. This appraoch combines a local surface inclination method and deep learning. Deep-learning flowfield prediction has been employed to predict surface flow profiles of the vehicle fuselage and scramjet engine over various angle of attack and injection conditions while local surface inclination has been applied for evaluating the other component of vehicles such as a main wing and a vartical tail.

Multi-objective design optimization of hypersonic airbreathing vehicle has been conducted using the developed evaluation appraoch and an evolutionary algorithm. Deisng parameters of both vehicle and scramjet geometires have simultaneously been optimized to maximize lift coefficient and to minimize the fuel consumption for cruise. Control parameters (angle of attack and injection pressure) for the trim flight have been determined through gradient-based optimization. It has been found that the cruise angle of attack and injection pressure are responsible for the variations of objective function values among the non-dominated solutions, whereas the geometries are similar to each other. Aerodynamic coefficients over angle of attack and injection pressure have been displayed indicating that the present optimization framework has successfully explore feasible design of hypersonic vehicle considering the effect of engine operation.

The present study have proposed a new appraoch to design hypersonic airbreathing vehicle. While a simple wedge-shape waverider has been considered as the design target of the present study, further

research will be conducted to extend the applicability of this approach to enable more global design exploration.

References

- [1] Taguchi, H., Murakami, A., Sato, T., and Tsuchiya, T., "Conceptual Study on Hypersonic Turbojet Experimental Vehicle (HYTEX)," *Transactions of JSASS*, Vol.7, No.ists26, pp.27-32, 2009.
- [2] Taguchi, H., Kobayashi, H., Kojima, T., Ueno, A., Imamura, S., Hongoh M., and Harada, K., "Research on hypersonic aircraft using pre-cooled turbojet engines," *Acta Astronaut.*, Vol.73, pp.164-172, 2012.
- [3] Preller, D. and Smart, M.K., "Reusable Launch of Small Satellites Using Scramjets," *J. Spacecr. Rockets*, Vol.54, No.6, pp.1317-1329, 2017.
- [4] Bowcutt, K.G., "Multidisciplinary Optimization of Airbreathing Hypersonic Vehicles," *J. Propuls. Power*, Vol.17, No.6, pp.1184-1190, 2001.
- [5] Riggins, D.W., Camberos, J., Wolff, M., and Bowcutt, K., "Mission-Integrated Exergy Analysis for Hypersonic Vehicles: Methodology and Application," J. Propuls. Power, Vol.29, No.3, pp.610-620, 2013.
- [6] Dalle, D.J., Torrez, S.M., Driscoll, J.S., Bolender, M.A., and Bowcutt, K.G., "Minimum-Fuel Ascent of a Hypersonic Vehicle Using Surrogate Optimization," *J. Aircr.*, Vol.51, No.6, pp.1973-1986, 2014.
- [7] Morita, N. and Tsuchiya, T., "Validations and Applications to Hypersonic Aircraft of 3D Unstructured Panel Method and Shell FEM for Optimizations," 56th Annual Aircraft Symposium, Yamagata, Japan, 2018.
- [8] Robert A. McDonald and James R. Gloudemans. "Open Vehicle Sketch Pad: An Open Source Parametric Geometry and Analysis Tool for Conceptual Aircraft Design," AIAA 2022-0004. AIAA SCITECH 2022 Forum. January 2022
- [9] Fujio, C. and Ogawa, H., "Deep-learning prediction and uncertainty quantification for scramjet intake flowfields," *Aerosp. Sci. Technol.*, Vol.130, p.107931, 2022.
- [10] Fujio, C. and Ogawa, H., "Sensitivity analysis for knowledge discovery in scramjet intake design optimization using deep-learning flowfield prediction," *Aerosp. Sci. Technol.*, Vol.150, p.109183, 2024.
- [11] Fujio, C. and Ogawa, H., "Optimization and data mining for shock-induced mixing enhancement inside scramjet using stochastic deep-learning flowfield prediction," *Aerosp. Sci. Technol.*, Vol.154, p.109513, 2024.
- [12] Kingma, D.P. and Ba, J., "Adam: A Method for Stochastic Optimization," the 3rd International Conference for Learning Representations, San Diego, May, 2015
- [13] Menter, F.R., "Two-equation eddy-viscosity turbulence models for engineering applications," *AIAA J.*, Vol.32, No.8, pp.1598-1605, 1994.
- [14] Boivin, P., Jiménez, C., Sánchez, A.L., and Williams, F.A., "An explicit reduced mechanism for H2–air combustion," *Proc. Combust. Inst.*, Vol.33, No.1, pp.517-523, 2011.
- [15] K. Deb, A. Pratap, S. Agarwal and T. Meyarivan, "A fast and elitist multiobjective genetic algorithm: NSGA-II," *IEEE Trans. Evol. Comput.*, vol.6, No.2, pp.182-197,2002